Dark Z implication for flavor physics

Fanrong Xu

Institute of Physics, Academia Sinica,
Taipei, Taiwan 11529, R.O. China

Department of Physics, Jinan University,
Guangzhou 510632, P.R. China

Kavli Institute for Theoretical Physics China, Chinese Academy of Sciences,
Beijing 100190, P.R. China

E-mail: frxu@hep1.phys.ntu.edu.tw

ABSTRACT: Dark Z/dark photon (Z') is one candidate of dark force carrier, which helps to interpret the properties of dark matter (DM). Other than conventional studies of DM including direct detection, indirect detection and collider simulation, in this work we take flavor physics as a complementary approach to investigate the features of dark matter. We give an exact calculation of the new type of penguin diagram induced by Z' which further modifies the well-known X, Y, Z functions in penguin-box expansion. The measurement of rare decays $B \to K^{(*)}\mu^+\mu^-$ and $B_s \to \mu^+\mu^-$ at LHC, together with direct CP violation ε'/ε in $K \to \pi\pi$ as well as $K_L \to \mu^+\mu^-$, are used to determine the parameter space. The size of coupling constant, however, is found to be $\mathcal{O}(1)$ which is much weaker than the known constraints.

Contents

1 Introduction

Dark matter (DM) constitutes about 27% of the energy-matter budget of universe, significantly more than 5% of baryonic matter [1]. Nevertheless, the exact nature of DM is kept mysterious so far. Yet it is still unclear whether DM can be described by scalar, fermion, vector or even graviton.

Among various DM candidates, dark photon has been the one of particular interest. The idea was initialed in 1980s [2], and developed in recent years [3–15]. Suppose there is an extra U(1)$_D$ group besides SM gauge group, under which all the SM interactions are invariant. The gauge boson of U(1)$_D$, named dark photon, interacts with SM U(1)$_Y$ gauge boson via a kinetic mixing term. It helps to explain the astrophysical observation of positron excesses [16], as well as other astrophysical phenomenology such as supernova bounds [17] and Big Bang Nucleosynthesis [18]. The direct search of dark photon, for example XENON 100, has put a very strong constraint [19]. For $e^+ e^-$ collider, a recent search performed at BaBar shows a null result, neither finds nor rules out dark photon [20]. A further experiment, the Heavy Photon Search (HPS) experiment located at Jefferson Lab [21], is designed to search dark photon in the mass range 20 MeV to 1 GeV as well as the related coupling. However, it has been realized recently that a simple dark photon is

not favored by 3.6σ deviation of muon anomalous magnetic moment [22]. Given the fact that dark photon model is the extreme case when the parameter to describe Z-Z' mass mixing is closed in a more generic dark Z model, it is necessary to extend dark photon to dark Z which is the working frame of this paper.

Flavor physics is not only taken as a platform for precise test of SM, but also plays an important role in indirect search of new physics (NP) beyond Standard Model (SM). Great progresses have already been made since LHC runs. For example, it was hoped for decades that NP might exist in zero crossing point q_0^2 of the differential branching ratio of $B \to K^* \mu^+ \mu^-$ (see for example [23]) but finally turned out tiny NP effect [24]. Taken DM theory as one kind of ordinary NP theory, flavor physics then would provide as a complementary way for conventional approaches of DM study, including direct detection, indirect detection and collider production. Based on the great achievement made in Run I, the LHC has already started its Run II in 2015. Then it would be interesting, and timely, to connect together these two different fields, dark matter and flavor physics. A similar effort can also be found in [25].

The paper is organized as follows. In section 2, we will briefly set up the dark Z model. An exact result of Z' penguin and further modifications to X, Y, Z functions are given in section 3. Some typical processes which are affected by the Z' including the recently measured $B \to K^* \mu^+ \mu^-$ and $B_s \to \mu^+ \mu^-$, as well as ε'/ε and $K_L \to \mu^+ \mu^-$ are discussed in section 4, also the relevant formulas are given therein. In section 5 the obtained numerical results are shown, based on which we will make a discussion. The details of Z' penguin calculation can be found in appendix.

2 The model

Suppose there exits an extra U(1) group, other than SM U(1), what it brings in phenomenology is an interesting question. It was considered how electromagnetic charge is shifted by this extra U(1) group in the initial paper [2]. Until recently it becomes popular to take this U(1) gauge boson as a DM candidate.

Under the dark group, notated as $U(1)_D$, all the SM interactions are invariant. The connection between dark photon with SM particles is from a kinetic mixing term, leading to the effective Lagrangian [15]

$$\mathcal{L} = -\frac{1}{4}\hat{B}_{\mu\nu}\hat{B}^{\mu\nu} + \frac{1}{2}\frac{\epsilon}{\cos\theta_W}\hat{B}_{\mu\nu}\hat{Z}'^{\mu\nu} - \frac{1}{4}\hat{Z}'_{\mu\nu}\hat{Z}'^{\mu\nu}, \tag{2.1}$$

where θ_W is Weinberg angle, $\hat{Z}'$ and $\hat{B}$ are dark photon and SM B field with the corresponding field strength

$$\hat{B}_{\mu\nu} = \partial_\mu \hat{B}_\nu - \partial_\nu \hat{B}_\mu, \qquad \hat{Z}'_{\mu\nu} = \partial_\mu \hat{Z}'_\nu - \partial_\nu \hat{Z}'_\mu, \tag{2.2}$$

and the mixing of gauge bosons is mimicked by parameter ϵ, which is supposed to be small and need to be determined. The convention above, in gauge interaction state, is not

diagonalized. By redefining fields as

$$\begin{pmatrix} Z_0' \\ B \end{pmatrix} = \begin{pmatrix} \sqrt{1 - \frac{\epsilon^2}{c_W^2}} & 0 \\ -\frac{\epsilon}{c_W} & 1 \end{pmatrix} \begin{pmatrix} \hat{Z}' \\ \hat{B} \end{pmatrix}, \tag{2.3}$$

the Lagrangian is then rotated to a diagonal form

$$\mathcal{L} = -\frac{1}{4} B_{\mu\nu} B^{\mu\nu} - \frac{1}{4} Z'_{0,\mu\nu} Z_0'^{\mu\nu}. \tag{2.4}$$

Note here the field after rotation with a subscript 0 differs from the one before rotation with a hat. In SM the B field can be projected to photon and Z after spontaneous symmetry breaking (SSB). Incorporating Z_0', the related neutral gauge fields are shifted,

$$A = \hat{A} - \epsilon \hat{Z}_0'$$
$$Z_0 = \hat{Z}_0 + \epsilon \tan\theta_W \hat{Z}_0$$
$$Z_0' = \hat{Z}_0'. \tag{2.5}$$

The rotation does not change the definition of Z_0', however, photon and Z field are modified indeed. Due to this modification of gauge fields, the interaction between Z_0' and ordinary matter is induced, which is named as dark photon model.

When Z_0'-Z_0 mass mixing is considered, the simple dark photon model is then extended to dark Z model. Generally speaking, the mass of Z' could either be added by hand which is called Stückelberg mechanism [26] (the origin of Stückelberg photon, for example, is discussed in string theory [27]) or by applying Higgs mechanism, see [15] as an example. In this paper, we shall adopt the treatment of Z' mass in the latter case, without involving the details of the mechanism itself. After the neutral gauge bosons obtain mass after SSB, a further rotation is required after the one in eq. (2.3) for diagonalising mass matrix

$$\begin{pmatrix} Z \\ Z' \end{pmatrix} = \begin{pmatrix} \cos\zeta & -\sin\zeta \\ \sin\zeta & \cos\zeta \end{pmatrix} \begin{pmatrix} Z_0 \\ Z_0' \end{pmatrix} \tag{2.6}$$

where the rotation angle ζ is model dependent and analytically might be complicated, but numerically should be small, (for example, see [15]). Now combine together the two rotations eq. (2.3) and eq. (2.6), the modifications to photon and Z by dark Z shows

$$A_\mu = \hat{A}_\mu - \epsilon Z'_\mu \tag{2.7a}$$
$$Z_\mu = \cos\zeta \hat{Z}_{0,\mu} - \epsilon_Z Z'_\mu \approx \hat{Z}_{0,\mu} - \epsilon_Z Z'_\mu. \tag{2.7b}$$

Formally the shift of neutral fields in dark photon model is characterised by two independent parameters ϵ and ϵ_Z, respectively. In fact ϵ_Z also has a lengthy analytical expression based on detailed model. The equivalent ϵ_Z defined to replace the complicated structure brings the convenience. The dark Z field here and also hereafter is denoted as Z', with original SM field denoted with a hat. The two coupling constants together with Z' mass constitute the unique 3 model parameters of dark Z, which could be measured in experiments.

Apparently the interactions between Z' and SM particles are simply induced by the shifted neutral gauge field. Explicitly, we show how Z' couples to SM fermions,

$$\mathcal{L}_{Z'ff} = -\left(\epsilon e J^\mu_{\text{em}} + \epsilon_Z \frac{g}{2\cos\theta_W} J^\mu_{\text{NC}}\right) Z'_\mu \tag{2.8}$$

in which the SM electrical current and weak neutral current are

$$J^\mu_{\text{em}} = Q_f \bar{f}\gamma^\mu f\,,$$
$$J^\mu_{\text{NC}} = (T_{3f} - 2Q_f \sin^2\theta_W)\bar{f}\gamma^\mu f - T_{3f}\bar{f}\gamma^\mu\gamma_5 f\,, \tag{2.9}$$

where f stands for fermions with corresponding electric charge Q_f, isospin $T_{3f} = \pm\frac{1}{2}$. With both vector coupling and axial-vector coupling, Z' behaves as a light version of Z and heavier version of photon. For the coupling of Z' and other gauge bosons, it has both "Z component" and "A component" sized by ϵ and ϵ_Z respectively.

3 The Z' effect in FCNC processes

As current energy frontier, the LHC brings plentiful opportunities for flavour physics which dominated by flavour changing neutral current (FCNC) processes. In this section, we will investigate these processes of meson physics in dark Z model. It is known in SM FCNC processes are induced at loop level. Conventionally the Feynman diagrams contributing to FCNC can be classified to three point penguin diagram and four point box diagram. If NP exists, the new interaction brought in by NP will modify parts/all of these SM penguin and box contribution. Within the Z' model working frame, however, this modification is only applied in photon penguin and Z penguin, keeping box diagram contribution unchanged. To make the new effect more distinguishable, we extract these modifications alone and name it as Z'-penguin specifically.

3.1 Z' penguin

We take $b \to sZ'$ as an example, noting similar result can be applied to $b \to dZ'$ and $s \to dZ'$ when necessary conditions are satisfied.

In Feynman-t' Hooft gauge there are totally 10 Feynman diagrams giving contributions to $b \to sZ'$. During our realistic calculation, we group two of the external leg corrections and replace them by an effective vertex shown in figure 1, with Z' inserted in either two legs. The four self-energy diagrams, effectively two, are then shown as (g) in figure 2, together with the remaining six ordinary three point diagrams given as (a) to (f).

As mentioned above the full result can be decomposed into "A component" (or ϵ component) and "Z component" (or ϵ_Z component). The ϵ component is same as $b \to s\gamma$ while the latter one is similar to $b \to sZ$. For photon penguin, there are two types of effective verteices corresponding to real and virtual photon. In below since we focus on semileptonic processes thus only the virtual photon vertex is taken into account. In order to keep the final result the same structure as photon penguin, the ϵ_Z component differs
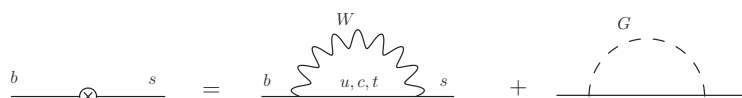
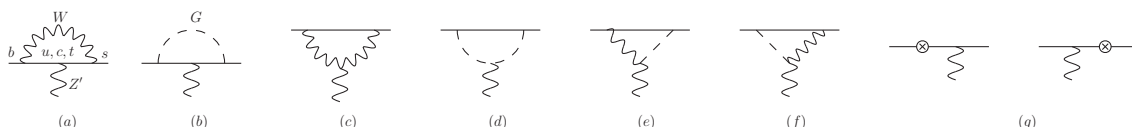**Figure 1**. The effective vertex for $b \to s$ transition.

Figure 2. The Feynman diagrams contributing to $b \to sZ'$ in Feynman-t' Hooft gauge. Figure (a) to (f) are three point diagrams while figure (g) is from the correction to external leg where the effective vertex denoted by a cross is explained in figure 1.

from SM Z penguin by neglecting dipole term contribution. An exact calculation, shown in appendix A, gives the Z' penguin vertex as

$$\overline{s}\Gamma^\mu b\big|_{Z'} = i\lambda_i \frac{G_F}{\sqrt{2}} \frac{e}{8\pi^2} H_0(x_i)\overline{s}(q^2\gamma^\mu - q^\mu q\!\!\!/)(1 - \gamma_5)b \,, \tag{3.1}$$

in which $\lambda_i = V_{ib}V_{is}^*$ $(i = u, c, t)$, $x_i = \frac{m_i^2}{m_W^2}$ and q is outgoing momentum carried by gauge boson. The vertex function $H_0(x_i)$ consisting of photon component function $D_0(x_i)$ and newly calculated Z component function $\tilde{D}_0(x_i)$, are characterised by ϵ and ϵ_Z, giving

$$H_0(x) = \epsilon D_0(x) + \epsilon_Z \tilde{D}_0(x) \tag{3.2a}$$

$$D_0(x) = -\frac{4}{9}\ln x + \frac{-19x^3 + 25x^2}{36(x-1)^3} + \frac{x^2(5x^2 - 2x - 6)}{18(x-1)^4}\ln x \tag{3.2b}$$

$$\tilde{D}_0(x) = -\frac{1}{s_W c_W}\left[\frac{34x^3 - 141x^2 + 147x - 58}{216(-1)^3} + \frac{(-3x^4 + 18x^3 - 27x^2 + 19x - 4)\ln x}{36(x-1)^4}\right.$$
$$\left. + c_W^2\left(\frac{-47x^3 + 237x^2 - 312x + 104}{108(x-1)^3} + \frac{(3x^4 - 30x^3 + 54x^2 - 32x + 8)\ln x}{18(x-1)^4}\right)\right], \tag{3.2c}$$

with $s_W = \sin\theta_W, c_W = \cos\theta_W$. Note during evaluating, the light down type quark is supposed to be massless and the momentum transfer is small, comparable to light quark mass. We also assume the light Z' mass smaller than the mass threshold for muon pair production, which guarantees no Z' resonance is produced when final state of charged lepton is muon. Also in this work we will not touch electron and neutrino as the lepton final state for the production of Z' when $m_{Z'}$ is above electron threshold. Nevertheless, it is safe to neglect $m_{Z'}$ in this paper.

3.2 The modification to X, Y, Z function

In the state-of-the-art effective Hamiltonian approach, physical observables can be factorized into short distance (SD) and long distance (LD) contribution. The SD part is

treated in perturbative theory while LD hadronic matrix resorts to various methods including lattice QCD. The SD contribution gives various combination of penguin diagrams and box diagrams and leads to he so-called X, Y, Z functions, which also depends on both the theoretical working frame and the calculated physical observable. For example, Y is to characterize the Wilson coefficient in the effective Hamiltonian of $B_q \to \ell^+\ell^-$, and for a more complicated process $B \to K^*\mu^+\mu^-$ more functions are involved. In the frame of Z' model, we have already discussed a new Z' penguin in previous sector. Before combining detailed phenomenology, to include Z' contribution in standard X, Y, Z functions systematically is now our target,

In SM the X, Y, Z functions are obtained via combing $bs\gamma$, bsZ, box diagram vertex (see [28]), and now we need to contain bsZ' vertex. The amplitudes of $b \to s\bar{\ell}\ell$ (or $\bar{s}b \to \bar{\ell}\ell$) mediated by different gauge bosons are in the form of

$$i\mathcal{M}_\gamma = i\lambda_i \frac{G_F}{\sqrt{2}} \frac{\alpha}{2\pi} D_0(x_i)(\bar{s}b)_{V-A}(\bar{\ell}\ell)_V \tag{3.3}$$

$$i\mathcal{M}_Z = i\lambda_i \frac{G_F}{\sqrt{2}} \frac{\alpha}{2\pi s_W^2} 2C_0(x_i)\big[v_f(\bar{s}b)_{V-A}(\bar{L}L)_V - a_f(\bar{s}b)_{V-A}(\bar{L}L)_A\big]$$

$$i\mathcal{M}_{Z'} = i\lambda_i \frac{G_F}{\sqrt{2}} \frac{\alpha}{2\pi s_W^2} 2C_0(x_i)\left[\frac{s_W H_0(x_i)}{4c_W C_0(x_i)} v'_f(\bar{s}b)_{V-A}(\bar{L}L)_V - \frac{s_W H_0(x_i)}{4c_W C_0(x_i)} a'_f(\bar{s}b)_{V-A}(\bar{L}L)_A\right]$$

with $L = (\ell, \nu)$ and the coupling of Zff and $Z'ff$

$$\begin{aligned} v_f &= T_{3f} - 2Q_f s_W^2, & a_f &= T_{3f}, \\ v'_f &= \epsilon \cdot 2Q_f s_W c_W + \epsilon_Z(T_{3f} - 2Q_f s_W^2), & a'_f &= \epsilon_Z T_{3f}. \end{aligned} \tag{3.4}$$

For convenience Z and Z' contribution can be put together in a compact form by showing exact final state

$$i\mathcal{M}_{ZZ'}^{\bar{\ell}\ell} = i\lambda_i \frac{G_F}{\sqrt{2}} \frac{\alpha}{2\pi s_W^2} C_0(x_i)\big[(-1 + 4s_W^2)(1 + \delta_1)(\bar{s}b)_{V-A}(\bar{\ell}\ell)_V + (1 + \delta_2)(\bar{s}b)_{V-A}(\bar{\ell}\ell)_A\big]$$

$$i\mathcal{M}_{ZZ'}^{\bar{\nu}\nu} = i\lambda_i \frac{G_F}{\sqrt{2}} \frac{\alpha}{2\pi s_W^2} C_0(x_i)\big[(1 + \delta_2)(\bar{s}b)_{V-A}(\bar{\nu}\nu)_V - (1 + \delta_2)(\bar{s}b)_{V-A}(\bar{\nu}\nu)_A\big] \tag{3.5}$$

in which we have introduced two parameters

$$\delta_1 = \frac{s_W H_0(x_i)}{4c_W C_0(x_i)}\left[\epsilon \frac{4c_W s_W}{1 - 4s_W^2} + \epsilon_Z\right], \qquad \delta_2 = \epsilon_Z \frac{s_W H_0(x_i)}{4c_W C_0(x_i)}. \tag{3.6}$$

Incoperating box diagram contribution, the Wilson coefficients of operators $Q_9^{\bar{\ell}\ell} = (\bar{s}b)_{V-A}(\bar{\ell}\ell)_V$, $Q_{10}^{\bar{\ell}\ell} = (\bar{s}b)_{V-A}(\bar{\ell}\ell)_A$ as well as quark-neutrino operator $Q_{V-A}^{\bar{\nu}\nu} = (\bar{s}b)_{V-A}(\bar{\nu}\nu)_{V-A}$ can be explicitly extracted as

$$C_9^{\bar{\ell}\ell} = \lambda_i \frac{G_F}{\sqrt{2}} \frac{\alpha}{2\pi s_W^2}\big[s_W^2 \cdot 4\big(Z_0(x_i) + \Delta Z_0(x_i)\big) - \big(Y_0(x_i) + \Delta Y_V(x_i)\big)\big]$$

$$C_{10}^{\bar{\ell}\ell} = \lambda_i \frac{G_F}{\sqrt{2}} \frac{\alpha}{2\pi s_W^2}\big[Y_0(x_i) + \Delta Y_A(x_i)\big] \tag{3.7}$$

$$C^{\bar{\nu}\nu} = \lambda_i \frac{G_F}{\sqrt{2}} \frac{\alpha}{2\pi s_W^2}\big[X_0(x_i) + \Delta X_0(x_i)\big]$$

in which the X, Y, Z functions are given in the combination of penguin and box diagrams $X_0(x) = C_0(x) - 4B_0(x)$, $Y_0(x) = C_0(x) - B_0(x)$, $Z_0(x) = C_0(x) + \frac{1}{4}D_0(x)$. The corresponding corrections to X, Y, Z are then given as

$$\Delta Y_V(x) = \delta_1 C_0(x), \qquad\qquad \Delta Z_0(x) = \delta_1 C_0(x), \qquad (3.8a)$$

$$\Delta X_0(x) = \delta_2 C_0(x), \qquad\qquad \Delta Y_A(x) = \delta_2 C_0(x). \qquad (3.8b)$$

Especially, we find that the modification to Y has two types due to different Dirac structure of lepton pair in the operators, while modification to X and Z function are in a fixed way. The modifications can be written in a more explicit form as

$$\Delta X_0(x) = \frac{1}{4} t_W \epsilon_Z H_0(x) \qquad (3.9a)$$

$$\Delta Y_A(x) = \frac{1}{4} t_W \epsilon_Z H_0(x) \qquad (3.9b)$$

$$\Delta Y_V(x) = \left[\epsilon \frac{s_W^2}{1 - 4s_W^2} + \epsilon_Z \frac{t_W}{4} \right] H_0(x) \qquad (3.9c)$$

$$\Delta Z_0(x) = \left[\epsilon \frac{s_W^2}{1 - 4s_W^2} + \epsilon_Z \frac{t_W}{4} \right] H_0(x). \qquad (3.9d)$$

In the limit of $\epsilon \to 0$, $\delta_1 = \delta_2$, the modifications are identical. However, if $\epsilon_Z \to 0$ (exactly dark photon model case), leading to $\Delta X_0 = \Delta Y_A = 0$, then the phenomenology is much more tedious.

4 Phenomenology

The physical observables can be classified into two types in dark Z model. One type relating to box diagram, like the mass difference of neutral meson, is not modified by Z'. The other one involving photon and Z penguins, such as the direct CP violation in $K \to \pi\pi$, does change. In this section, we will choose several typical processes to see a generic effect of Z' on flavour physics.

4.1 $B_q \to \mu^+\mu^-$

It has been hoped for decades that NP might be unfolded in rare decay $B_s \to \mu^+\mu^-$. However, no hint of NP appeared in $B_s \to \mu^+\mu^-$ mode from LHC Run I data, given by the full combination results of CMS and LHCb [29]

$$\mathcal{B}(B_s \to \mu^+\mu^-) = (2.8^{+0.7}_{-0.6}) \times 10^{-9} \qquad (4.1a)$$

$$\mathcal{B}(B_d \to \mu^+\mu^-) = (3.9^{+1.6}_{-1.4}) \times 10^{-10}. \qquad (4.1b)$$

Though $B_s \to \mu^+\mu^-$ turns out to be SM-like, there remains a hope for NP in the much rarer mode $B_d \to \mu^+\mu^-$ (for example, see [30]).

Due to the precise measurement of decay $B_s \to \ell^+\ell^-$ is now realistic, one should consider the effect of sizeable width difference $\Delta\Gamma_s$ in B_s^0-$\overline{B}_s^0$ oscillation. The theoretical

formula has to be corrected to compare with measured branching ratio [31, 32] which is denoted with a bar,

$$\mathcal{B}(B_s^0 \to \ell^+\ell^-) = \left[\frac{1 - y_s^2}{1 + \mathcal{A}_{\Delta\Gamma}^{\ell^+\ell^-} y_s}\right]\overline{\mathcal{B}}(B_s^0 \to \ell^+\ell^-) \tag{4.2}$$

where $y_s \equiv \frac{\Delta\Gamma_s}{2\Gamma_s} \equiv \frac{\Gamma_L^{(L)} - \Gamma_L^{(s)}}{2\Gamma_s}$, $\mathcal{A}_{\Delta\Gamma}^{\ell^+\ell^-} = \frac{R_H^{\ell^+\ell^-} - R_L^{\ell^+\ell^-}}{R_H^{\ell^+\ell^-} + R_L^{\ell^+\ell^-}}$. It is known $\mathcal{A}_{\Delta\Gamma}^{\ell^+\ell^-} = 1$ in SM [32], thus

$$\mathcal{B}(B_s^0 \to \ell^+\ell^-) = (1 - y_s^2)\overline{\mathcal{B}}(B_s^0 \to \ell^+\ell^-). \tag{4.3}$$

The latest estimation of parameter y_s is $y_s = 0.069 \pm 0.006$ given in [35]. Note in the dark photon model, the relation of eq. (4.3) does not change. While for the rarer $B_d \to \ell^+\ell^-$ decay, the effect from oscillation in B^0-$\overline{B}^0$ can be neglected thus we do not take this correction.

The (uncorrected) SM branching ratio of $B_q \to \ell^+\ell^-$ is induced by Z penguin and hence depends on Q_{10}, (see ref. [36]). Now incorporating Z'-penguin, which gives a similar component as Z, leads to

$$\mathcal{B}(B_q \to \ell^+\ell^-) = \tau(B_q)\frac{G_F^2}{\pi}\left(\frac{\alpha}{4\pi s_W^2}\right)^2 f_B^2 m_\ell^2 m_B \sqrt{1 - \frac{4m_\ell^2}{m_B^2}}\,\eta_{\text{eff}}^2 \big|\lambda_t\big(Y_0(x_t) + \Delta Y_A(x_t)\big)\big|^2 \tag{4.4}$$

with $\eta_{\text{eff}} = 0.9882 \pm 0.0024$ which takes into account NNLO QCD correction and NLO electroweak correction [36]. Apparently the reason why only ΔY_A contributes, is exact with the same reason why photon penguin contribution vanishes.

4.2 $B \to K^{(*)}\mu^+\mu^-$

The quest for NP in $B \to K^{(*)}\mu^+\mu^-$ has been performed for a long time. In the beginning the zero crossing-point q_0^2 is of the first priority, however, q_0^2 turns out to be compatible with SM prediction finally from the released LHC data. The remaining possibility for NP in this mode, the P_5' problem, requires more data to confirm. Meanwhile for the $B \to K\ell^+\ell^-$ channel, there is a NP hint, so called R_K problem, which violates lepton universality.

The theoretical study for this channel has been developed for around 30 years, including multi-loop calculation of Wilson coefficients at high energy. The most matured theoretical treatment in low energy to the semileptonic decays are based on QCDF. It is not necessary to repeat the whole long story in this work. Instead, we would like to simply focus on C_9 and C_{10} to see how the data constrain the NP parameter space. In dark Z model, the modification of C_9 and C_{10} due to the dark Z contribution is

$$\Delta C_9(x_i) = 4\Delta Z_0(x_i) - \frac{\Delta Y_V(x_i)}{s_W^2} \tag{4.5a}$$

$$\Delta C_{10}(x_i) = \frac{\Delta Y_A(x_i)}{s_W^2}. \tag{4.5b}$$

Driven by new data many efforts have been made to extract the information hidden inside the two coefficients. In [37] a model-independent fit was taken based on $B \to X_s\ell^+\ell^-$,

$B \to X_s\gamma$, $B \to K^*\gamma$ and $B \to K^*\mu^+\mu^-$, we will adopt their constraints on ΔC_9 and ΔC_{10} at 2σ[1]

$$-1.5 < \text{Re}(\Delta C_9) < 1.2, \qquad\qquad -2.8 < \text{Im}(\Delta C_9) < 2.8 \qquad (4.6a)$$
$$-1 < \text{Re}(\Delta C_{10}) < 1.5, \qquad\qquad -3 < \text{Im}(\Delta C_{10}) < 3. \qquad (4.6b)$$

In our scenario, the NP only exists in the change of real part of $C_{9/10}$.

4.3 $K_L \to \mu\bar{\mu}$

The branching ratio of $K_L \to \mu\bar{\mu}$ contains LD and SD contribution. The calculation of LD contribution remains a challenge in theory. Combining a latest theoretical LD estimation and experimental bound [39],[2] the constraint to SD is

$$\mathcal{B}(K_L \to \mu^+\mu^-)_{\text{SD}} \le 2.5 \times 10^{-9}. \qquad (4.7)$$

The branching ratio from SD (see ref. [40])

$$\mathcal{B}(K_L \to \mu^+\mu^-)_{\text{SD}} = \kappa_\mu \left[\frac{\text{Re}(\lambda_c)}{|V_{us}|} P_c(Y_K) + \frac{\text{Re}(\lambda_t)}{|V_{us}|^5} \eta_Y Y_0(x_t) \right]^2$$

with $\lambda_q = V_{qs}^* V_{qd}$ $(q = c, t)$ and $\kappa_\mu = (2.009 \pm 0.017) \times 10^{-9} \left(\frac{|V_{us}|}{0.225}\right)^8$, $P_c(Y_K) = (0.115 \pm 0.018)\left(\frac{0.225}{|V_{us}|}\right)^8$ [41], QCD correction factor $\eta_Y = 1.012$ [42], now is modified as

$$\mathcal{B}(K_L \to \mu^+\mu^-)_{\text{SD}} = \kappa_\mu \left[\frac{\text{Re}(\lambda_c)}{|V_{us}|} P_c(Y_K) + \frac{\text{Re}(\lambda_t)}{|V_{us}|^5} \eta_Y \big(Y_0(x_t) + \Delta Y_A(x_t)\big) \right]^2, \qquad (4.8)$$

by including the dark Z contribution.

4.4 $\frac{\varepsilon'}{\varepsilon}$

Historically two approaches, operator production expansion (OPE) method and penguin-box expansion (PBE) method, are adopted for the study of direct CP violation in $K \to \pi\pi$, which involves all the QCD penguin and electroweak penguin in SM. For the phenomenology study here, we make use of the simple analytical formula based on the PBE method [43]. By modifying relevant parts due to the dark Z effect, an updated formula[3] to depicted ε'/ε is

$$\text{Re} \frac{\varepsilon'}{\varepsilon} = a \, \text{Im}(\lambda_t) \cdot F(x_t) \qquad (4.9)$$

---

[1]Later in another independent analysis [38], the global fit combining $B \to X_s\ell^+\ell^-$, $B \to K^*\mu^+\mu^-$, $B \to K\mu^+\mu^-$ and $B_s \to \mu^+\mu^-$ together obtained a similar constraint on C_{10}.

[2]The SM prediction is then $\mathcal{B}(K_L \to \mu^+\mu^-)_{\text{SD}} = (0.79 \pm 0.12) \times 10^{-9}$, the experimental value in PDG is $\mathcal{B}(K_L \to \mu^+\mu^-)_{\text{exp.}} = (6.84 \pm 0.11) \times 10^{-9}$.

[3]We should keep in mind that the original formula was obtained by comparing with two methods in SM [43]. A more serious formula in dark Z model should be given by repeating this work similarly due to different types of ΔY, which is beyond the scope of current work. In the numerically study below, we will take ΔY_V as an example. However, we will understand the exact form of ΔY should keep the paper's conclusion.

where $F(x)$ is given by

$$F(x) = P_0 + P_X\big[X_0(x) + \Delta X(x)\big] + P_Y\big[Y_0(x) + \Delta Y(x)\big] + P_Z\big[Z_0(x) + \Delta Z\big] + P_E E_0(x) \tag{4.10}$$

and the factor $a = 0.92 \pm 0.03$ [44], which takes into account the correction due to $\Delta I = 5/2$ transitions [45]. Note the dark Z modifies most parts of SM F function but keep the gluon penguin vertex $E(x)$ unchanged. The coefficients P_i $(i = 0, X, Y, Z, E)$ are given in terms of R_6, R_8

$$P_i = r_0^{(0)} + r_i^{(6)} R_6 + r_i^{(8)} R_8 . \tag{4.11}$$

We adopt their numerical values for $\alpha_s(M_Z) = 0.1185$ [46] given in table 1 of ref. [44]. For the nonperturbative parameters,we adopt the value $R_8 = 0.6, R_6 = 1.1$. The former one is obtained from lattice [47], with the translation by ref. [44]. But a reliable lattice result for R_6 is still lack, here we choose 10% deviation from large N result. The experimental value with 1σ error for ε'/ε is

$$\frac{\varepsilon'}{\varepsilon} \simeq \mathrm{Re}\left(\frac{\varepsilon'}{\varepsilon}\right) = (1.66 \pm 0.23) \times 10^{-3}, \tag{4.12}$$

taken form PDG [46].

5 Results and discussion

There are limited three free parameters in dark Z model, $m_{Z'}$, ϵ and ϵ_Z. In our working scenario, the light Z' mass is ignored thus it might be promising to determine the remaining two by above observables. We take the global fit of Wolfenstein parametrization of CKM matrix as input since Z' does not change SM flavour structure. The other related input parameters have been given herebefore. Combining $B_s \to \mu^+\mu^-$, $K_L \to \mu^+\mu^-$ and ΔC_9, ΔC_{10} from a global fit of $B \to K^{(*)}\mu^+\mu^-$ and so on, we plot allowed parameter space in (ϵ, ϵ_Z) plane shown in figure 3.

The ranges of ϵ and ϵ_Z are both shown in the section $(-10, 10)$. Due to its large uncertainty SD of $K_L \to \mu^+\mu^-$, as presented in grey region, gives a pretty wide band with $\frac{3}{5}$ slope. The green band with the same slope and less width of grey one, together with the gap out of this band surrounded by a set of hyperbolic curve, is resulted from ΔC_{10}. Another parameter obtained from $B \to K^{(*)}\mu^+\mu^-$ samely, ΔC_9, constrains parameters in blue colour, which is restricted in two sets of hyperbolic curves and extended to slope $\frac{3}{5}$ direction as well as near vertical direction. Apparently the latter part is excluded by $K_L \to \mu^+\mu^-$ (or C_{10}) while the former one is embedding in green area. Remarking in orange, the important $B_s \to \mu^+\mu^-$ also embeds in ΔC_{10} but somehow has an overlap part with ΔC_9. In principle, $B_d \to \mu^+\mu^-$ can also be included. Considering its uncertainty is larger than $B_s \to \mu^+\mu^-$, the allowed region is then also wider than current orange area thus we do not show it. Here we also add in a typical constraint from ε'/ε by fixing its non-perturbative parameter R_6 and R_8. Showing as two narrow hyperbolic curves in yellow, it looks ε'/ε could give a very strict constraint. However, due to the large uncertainty of the two non-perturbative parameters, especially R_6, one cannot take the direct CP violation of
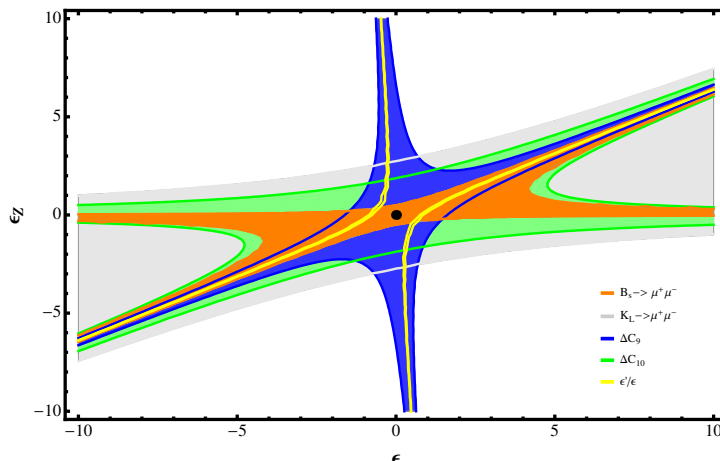
Figure 3. The allowed $\epsilon - \epsilon_Z$ parameter space by various experiments if $m_{Z'}$ is less than $2m_\mu$ and hence ignored. The meaning of colours are given as: grey stands for $K_L \to \mu^+\mu^-$, orange represents $B_s \to \mu^+\mu^-$, green denotes ΔC_{10}, blue stands for ΔC_9 while the yellow is one example of ε'/ε with $(R_6, R_8) = (0.7, 1.1)$ and the black dot remarkes SM case.

kaon too seriously. Nevertheless, once R_6 is fixed within certain precisement in the future, ε'/ε can be taken as an important discrimination to further constrain the parameter.

Aiming at the determination of parameter space of dark Z model, we reach the allowed (ϵ, ϵ_Z) in the narrow linear region

$$\epsilon_Z = \frac{3}{5}\epsilon \qquad (5.1)$$

and especially $-2 < \epsilon < 2$, $-1 < \epsilon_Z < 1$ are favored. In other words, the order of mixing parameters is constrained to be $\mathcal{O}(1)$. Generally speaking, more FCNC processes can be considered to determine the bound, but we can believe $\mathcal{O}(1)$ should be the typical value from flavour physics.

Many other works have already put constraints on dark photon model. Though it is not exact same model as our working scenario, the obtained mixing angle in dark photon still enlightens parameters in dark Z model. For example, based on supernova 1987A the limit on mixing angle could be $\mathcal{O}(10^{-12.5})$ for $m_{Z'} > 2m_e$ [17]. A recent work from direct detection experiments such as XENON10 and XENON100, for the absence of an ionization signal, puts a even more stringent limit on ϵ down to $\mathcal{O}(10^{-15})$. One may expect if ϵ_Z is added, the bound of ϵ will also be changed from astrophysical observables and direct detection experiements. Meanwhile, the working scenario in flavour physics can also be modified to allow Z' resonance production [15], leading to a possible different constraint on mixing parameters. In any case, given the bound from flavour physics in current scenario $\mathcal{O}(1)$, one may not expect a dramatical change (a more than 10 orders of magnitude) happens unnaturally.

In the existence of dark Z, we have investigated its effect in flavour physics especially by connecting the effect to the newly measured processes at LHC. However, the obtained bound, $\mathcal{O}(1)$, may not compete with the corresponding one in traditional dark matter study.

Acknowledgments

A The calculation of Z' penguin

The effective bsZ' vertex is in the form of

$$\Gamma_\mu(k_1, k_2) = e\lambda_i \frac{g_2^2}{2(4\pi)^2 m_W^2} \left[F_1(q_\mu \slashed{q} - q^2 \gamma_\mu)\mathbb{P}_L + F_2\, i\sigma_{\mu\nu}q^\nu m_b \mathbb{P}_R \right], \qquad (A.1)$$

which satisfies Ward Identity approximately in the limit of $m_{Z'} \to 0$. In the phenomenology study of this work, we only focus on F_1 contribution, which has the relation with H_0 in section 3.1

$$H_0(x) = -2F_1(x). \qquad (A.2)$$

For convenience, in following calculation the effective vertex (A.1) can be rewritten as

$$\Gamma^\mu(k_1, k_2) = e\lambda_i \frac{g_2^2}{2(4\pi)^2 m_W^2} \left[c_L T_L^\mu + c_b T_b^\mu + c_s T_s^\mu \right] \qquad (A.3)$$

by introducing $c_b = F_1 + F_2$, $c_s = F_2 - F_1$, $c_L = -F_2$ and $T_L^\mu = m_b^2 \gamma^\mu \mathbb{P}_L$, $T_b^\mu = \slashed{k}_1 k_1^\mu \mathbb{P}_L$, $T_s^\mu = \slashed{k}_1 k_2^\mu \mathbb{P}_L$. Particularly we have

$$F_1 = \frac{1}{2}(c_b - c_s). \qquad (A.4)$$

In the calculation, the F_1 function may be projected to

$$F_1 = \epsilon F_1|_\gamma + \epsilon_Z F_1|_Z \qquad (A.5)$$

Following we will evaluate F_1 component by component.

A.1 The ϵ component

The contribution of ϵ component is exactly same as $b \to s\gamma$ case. Here we recalculate the photon penguin contribution. In Feynman-t' Hooft gauge, with the approximation $m_s = 0$, $q^2 = 0$ and making use of quark on-shell condition as well as unitary CKM relation, we have the total contribution as

$$i\Gamma^\mu\big|_\gamma = ie\lambda_i \frac{g_2^2}{2(4\pi)^2} \sum_j \mathcal{M}_j^\mu\big|_\gamma \qquad (A.6)$$

with the individual amplitude from each diagram

$$\mathcal{M}_a\big|_\gamma = -\frac{4}{3}\Big[\big(-2C_{00} + m_t^2 C_0 - m_b^2(C_0 + 2C_1 + C_2 + C_{11} + C_{12})\big)T_L$$
$$+ 2(C_{11} + C_1)T_b + 2(C_0 + C_1 + C_2 + C_{12})T_s\Big] \tag{A.7}$$

$$\mathcal{M}_b\big|_\gamma = -\frac{2}{3}\frac{m_t^2}{m_W^2}\bigg[\Big(-2C_{00} + \frac{1}{2} + m_t^2 C_0 - m_b^2(C_{11} + C_1 + C_{12} + C_0)\Big)T_L$$
$$+ 2C_{11}T_b + 2(C_{12}-C_2)T_s\bigg]$$

$$\mathcal{M}_c\big|_\gamma = -\Big[\big(12C_{00} + m_b^2(3C_1 + 2C_2 + 2C_{11} + 2C_{12})\big)T_L$$
$$+ (4C_{11} + 2C_1)T_b + (4C_{21} - 2C_1 - 2C_2)T_s\Big]$$

$$\mathcal{M}_d\big|_\gamma = -\frac{m_t^2}{m_W^2}\Big[2C_{00}T_L + (2C_{11} + 3C_1 + C_0)T_b + (2C_{21} + C_1 + 2C_2 + C_0)T_s\Big]$$

$$\mathcal{M}_e\big|_\gamma = m_t^2 C_0 T_L$$

$$\mathcal{M}_f\big|_\gamma = (m_t^2 C_0 + m_b^2 C_1)T_L + 2C_2 T_s$$

$$\mathcal{M}_g\big|_\gamma = \frac{1}{3}\bigg[(B_0 + B_1)\Big(2 + \frac{m_t^2}{m_W^2}\Big) - \frac{m_t^2}{m_W^2}\big(B_0(m_b^2, m_W^2, m_t^2) - B_0(0, m_W^2, m_t^2)\big)\bigg]T_L$$

in which B_i, C_j $(i = 0, 1; j = 0, 1, 2, 11, 12, 21, 22)$ are Pasarrino-Veltman integrals [48], and the positions for variables are assigned as $B(m_b^2, m_W^2, m_t^2)$, $C_{a,b}(m_b^2, 0, 0, m_W^2, m_t^2, m_t^2)$ for a, b case, and $C_{c,d,e,f}(m_b^2, 0, 0, m_t^2, m_W^2, m_W^2)$ for c, d, e, f case. Note in the calculation, the light down type quark contribution in Goldstone-quark-quark vertex cannot be neglected.

The PV functions can be reduced into basic scalar function B_0, C_0, and we further perform Taylar expansion up to m_b^4. Sum up all the contribution together, we have

$$i\Gamma^\mu\big|_\gamma = ie\lambda_i \frac{g_2^2}{2(4\pi)^2 m_W^2}\bigg[\Big(-\frac{1}{3} - 2\Delta_\epsilon\Big)\frac{T_L}{m_b^2} + c_L T_L + c_b T_b + c_s T_s\bigg] \tag{A.8a}$$

$$c_L\big|_\gamma = \frac{x_t^2(2 - 3x_t)\ln x_t}{2(x_t - 1)^4} - \frac{22x_t^3 - 153x_t^2 + 159x_t - 46}{36(x_t - 1)^3} \tag{A.8b}$$

$$c_b\big|_\gamma = \frac{(3x_t^4 - 3x_t^3 + 36x_t^2 - 32x_t + 8)\ln x_t}{18(x_t - 1)^4} + \frac{19x_t^3 - 222x_t^2 + 165x_t - 34}{108(x_t - 1)^3} \tag{A.8c}$$

$$c_s\big|_\gamma = \frac{(-3x_t^4 + 57x_t^3 - 72x_t^2 + 32x_t - 8)\ln x_t}{18(x_t - 1)^4} + \frac{113x_t^3 - 696x_t^2 + 789x_t - 242}{108(x_t - 1)^3} \tag{A.8d}$$

The first term in eq. (A.8a) gives zero contribution after applying the unitary triangle relation $\sum_i \lambda_i \cdot \text{constant} = 0$. Also we have

$$c_b\big|_\gamma - c_s\big|_\gamma = \frac{(3x_t^4 - 30x_t^3 + 54x_t^2 - 32x_t + 8)\ln x_t}{9(x_t - 1)^4} + \frac{-47x_t^3 + 237x_t^2 - 312x_t + 104}{54(x_t - 1)^3}$$
$$= -2\Big(D_0(x_t) + \frac{26}{27}\Big) \tag{A.9}$$

$$F_1\big|_\gamma = -D_0(x_i) \tag{A.10}$$

in which $D_0(x_i)$ is vertex function of virtual photon in $b \to s\gamma$. Note in my calculation, the D_0, D_0' differs from the one in [28], up to a minus sign, for the different convention in QED vertex.

A.2   The ϵ_Z component

The total contribution for $b \to sZ$ is

$$i\Gamma^\mu\big|_Z = i\frac{g_2^2}{2(4\pi)^2}\frac{g_2}{c_W}\lambda_i \sum_j \Gamma^\mu_j\big|_Z \tag{A.11}$$

Compared with $b \to s\gamma$ case, we only need to recalculate figure (a) and figure (b),

$$
\begin{aligned}
\Gamma^\mu_a\big|_Z = {} & \frac{2}{3}s_W^2 \cdot 2\big\{\big[-2C_{00} + m_t^2 C_0 - m_b^2(C_{11} + C_{12} + 2C_1 + C_2 + C_0)\big]T_L^\mu \\
& + 2(C_{11} + C_1)T_b^\mu + 2(C_{12} + C_2 + C_1 + C_0)T_s^\mu\big\} \\
& - \frac{1}{2} \cdot 2\big\{\big[-2C_{00} - m_b^2(C_{11} + C_{12} + 2C_1 + C_2 + C_0)\big]T_L^\mu \\
& + 2(C_{11} + C_1)T_b^\mu + 2(C_{12} + C_2 + C_1 + C_0)T_s^\mu\big\}
\end{aligned} \tag{A.12a}
$$

$$
\begin{aligned}
\Gamma^\mu_b\big|_Z = {} & \frac{2}{3}s_W^2 \cdot \frac{m_t^2}{m_W^2}\Big\{\Big[-2C_{00} + \frac{1}{2} + m_t^2 C_0 - m_b^2(C_{11} + C_{12} + C_1 + C_0)\Big]T_L^\mu \\
& + 2C_{11}T_b^\mu + 2(C_{12} - C_2)T_s^\mu\Big\} \\
& - \frac{1}{2} \cdot \frac{m_t^2}{m_W^2}\big\{\big[m_t^2 C_0 - m_b^2(C_0 + C_1)\big]T_L^\mu - 2C_2 T_s^\mu\big\}
\end{aligned} \tag{A.12b}
$$

while the other contributions are obtained by the following replacement

$$
\begin{aligned}
\text{Figure } (c): \qquad & e \to g_2 c_W \\
\text{Figure } (d): \qquad & e \to g_2\frac{1 - 2s_W^2}{2c_W} \\
\text{Figure } (e),\ (f): \qquad & e \to -\frac{g_2 s_W^2}{c_W} \\
\text{Figure } (g): \quad -Q_b \to & -\left(-\frac{1}{2} + \frac{1}{3}s_W^2\right)
\end{aligned} \tag{A.13}
$$

with the same PV function convention as in $b \to s\gamma$ case.

In this work, since we only consider the $(q_\mu \slashed{q} - q^2 \gamma_\mu)$ term, thus only the coefficients of T_b^μ and T_s^μ are of interest. Especially they are listed individually,

$$
\begin{aligned}
m_W^2 \Gamma^\mu_a\big|_Z = {} & \left[\frac{-5x_t^2 + 22x_t - 5}{18(x_t-1)^3} + \frac{(1-3x_t)\ln x_t}{3(x_t-1)^4} + s_W^2\left(\frac{2(5x_t^2 - 22x_t + 5)}{27(x_t-1)^3} + \frac{4(3x_t-1)\ln x_t}{9(x_t-1)^4}\right)\right]T_b^\mu \\
& + \bigg[\frac{20x_t^2 - 7x_t - 7}{18(x_t-1)^3} - \frac{(6x_t^2 - 6x_t + 1)\ln x_t}{3(x_t-1)^4} \\
& + s_W^2\left(-\frac{2(20x_t^2 - 7x_t - 7)}{27(x_t-1)^3} + \frac{4(6x_t^2 - 6x_t + 1)\ln x_t}{9(x_t-1)^4}\right)\bigg]T_s^\mu
\end{aligned}
$$

$$m_W^2 \Gamma_b^\mu \big|_Z = s_W^2 \left(\frac{2(2x_t^2 - 7x_t + 11)}{27(1 - x_t)^3} + \frac{4x_t \ln x_t}{9(x_t - 1)^4} \right) T_b^\mu$$

$$+ \left[\frac{x_t(x_t - 3)}{4(x_t - 1)^2} + \frac{x_t \ln x_t}{2(x_t - 1)^3} + s_W^2 \left(\frac{x_t(11x_t^2 - 43x_t + 38)}{27(x_t - 1)^3} - \frac{2(3x_t - 4) \ln x_t}{9(x_t - 1)^4} \right) \right] T_s^\mu$$

$$m_W^2 \Gamma_c^\mu \big|_Z = \left[\frac{-17x_t^2 - 8x_t + 1}{18(x_t - 1)^3} + \frac{x_t^2(x_t + 3) \ln x_t}{3(x_t - 1)^4} + s_W^2 \left(\frac{17x_t^2 + 8x_t - 1}{18(x_t - 1)^3} - \frac{x_t^2(x_t + 3) \ln x_t}{3(x_t - 1)^4} \right) \right] T_b^\mu$$

$$+ \left[\frac{-38x_t^2 + 43x_t - 11}{9(x_t - 1)^3} + \frac{2x_t^2(4x_t - 3) \ln x_t}{3(x_t - 1)^4} \right.$$

$$\left. + s_W^2 \left(-\frac{2x_t^2(4x_t - 3) \ln x_t}{3(x_t - 1)^4} + \frac{38x_t^3 - 43x_t + 11}{9(x_t - 1)^3} \right) \right] T_s^\mu$$

$$m_W^2 \Gamma_d^\mu \big|_Z = \left[\frac{x_t(x_t^2 - 8x_t - 17)}{72(x_t - 1)^3} + \frac{x_t^2(x_t^2 - 3x_t + 6) \ln x_t}{12(x_t - 1)^4} \right.$$

$$\left. + s_W^2 \left(\frac{x_t(x_t^2 - 8x_t - 17)}{36(1 - x_t)^3} - \frac{x_t^2(x_t^2 - 3x_t + 6) \ln x_t}{6(x_t - 1)^4} \right) \right] T_b^\mu$$

$$+ \left[\frac{x_t(23x_t^2 - 22x_t - 13)}{72(x_t - 1)^3} - \frac{(x_t^2 + 3x_t - 6) \ln x_t}{12(x_t - 1)^4} \right.$$

$$\left. + s_W^2 \left(\frac{x_t(-23x_t^2 + 22x_t + 13)}{36(x_t - 1)^3} + \frac{x_t^2(x_t^2 + 3x_t - 6) \ln x_t}{6(x_t - 1)^4} \right) \right] T_s^\mu$$

$$m_W^2 \Gamma_e^\mu \big|_Z = 0$$

$$m_W^2 \Gamma_f^\mu \big|_Z = s_W^2 \left(-\frac{1 - 3x_t}{2(x_t - 1)^2} - \frac{x_t^2 \ln x_t}{(x_t - 1)^3} \right) T_s^\mu$$

$$m_W^2 \Gamma_g^\mu \big|_Z = 0$$

Sum up together, we have

$$c_b \big|_Z = \left[\frac{-35x_t^3 + 156x_t^2 - 213x_t + 20}{216(x_t - 1)^3} + \frac{(-3x_t^4 + 9x_t^3 - 18x_t^2 + 28x_t - 4) \ln x_t}{36(x_t - 1)^4} \right. \tag{A.14}$$

$$\left. + c_W^2 \left(\frac{19x_t^3 - 222x_t^2 + 165x_t - 34}{108(x_t - 1)^3} + \frac{(3x_t^4 - 3x_t^3 + 36x_t^2 - 32x_t + 8) \ln x_t}{18(x_t - 1)^4} \right) \right]$$

$$c_s \big|_Z = \left[\frac{-103x_t^3 + 438x_t^2 - 507x_t + 136}{216(x_t - 1)^3} + \frac{(3x_t^4 - 27x_t^3 + 36x_t^2 - 10x_t + 4) \ln x_t}{36(x_t - 1)^4} \right. \tag{A.15}$$

$$\left. + c_W^2 \left(\frac{113x_t^3 - 696x_t^2 + 789x_t - 242}{108(x_t - 1)^3} + \frac{(-3x_t^4 + 57x_t^3 - 72x_t^2 + 32x_t - 8) \ln x_t}{18(x_t - 1)^4} \right) \right]$$

Now we obtain the $\tilde{D}_0$ function as

$$c_b \big|_Z - c_s \big|_Z = 2 \left[\frac{34x_t^3 - 141x_t^2 + 147x_t - 58}{216(x_t - 1)^3} + \frac{(-3x_t^4 + 18x_t^3 - 27x_t^2 + 19x_t - 4) \ln x_t}{36(x_t - 1)^4} \right.$$

$$\left. + c_W^2 \left(\frac{-47x_t^3 + 237x_t^2 - 312x_t + 104}{108(x_t - 1)^3} + \frac{(3x_t^4 - 30x_t^3 + 54x_t^2 - 32x_t + 8) \ln x_t}{18(x_t - 1)^4} \right) \right].$$

$$\tilde{D}_0(x_i) \equiv -F_1 \big|_Z = \frac{1}{2s_W c_W} \left(c_b \big|_Z - c_s \big|_Z \right) \tag{A.16}$$

Take into account D_0 and $\tilde{D}_0$ together, the vertex function for Z' penguin H_0 is produced.

References

[1] PLANCK collaboration, P.A.R. Ade et al., *Planck 2013 results. I. Overview of products and scientific results*, *Astron. Astrophys.* **571** (2014) A1 [arXiv:1303.5062] [INSPIRE].

[2] B. Holdom, *Two* U(1)*'s and ϵ charge shifts*, *Phys. Lett.* **B 166** (1986) 196 [INSPIRE].

[3] P. Fayet, *Light spin 1/2 or spin 0 dark matter particles*, *Phys. Rev.* **D 70** (2004) 023514 [hep-ph/0403226] [INSPIRE].

[4] D.P. Finkbeiner and N. Weiner, *Exciting dark matter and the INTEGRAL/SPI 511 keV signal*, *Phys. Rev.* **D 76** (2007) 083519 [astro-ph/0702587] [INSPIRE].

[5] N. Arkani-Hamed, D.P. Finkbeiner, T.R. Slatyer and N. Weiner, *A theory of dark matter*, *Phys. Rev.* **D 79** (2009) 015014 [arXiv:0810.0713] [INSPIRE].

[6] S. Andreas, M.D. Goodsell and A. Ringwald, *Dark matter and dark forces from a supersymmetric hidden sector*, *Phys. Rev.* **D 87** (2013) 025007 [arXiv:1109.2869] [INSPIRE].

[7] J.-W. Cui, H.-J. He, L.-C. Lu and F.-R. Yin, *Spontaneous mirror parity violation, common origin of matter and dark matter and the LHC signatures*, *Phys. Rev.* **D 85** (2012) 096003 [arXiv:1110.6893] [INSPIRE].

[8] D. Fargion, M. Khlopov and C.A. Stephan, *Cold dark matter by heavy double charged leptons?*, *Class. Quant. Grav.* **23** (2006) 7305 [astro-ph/0511789] [INSPIRE].

[9] M.Y. Khlopov and C.A. Stephan, *Composite dark matter with invisible light from almost-commutative geometry*, astro-ph/0603187 [INSPIRE].

[10] J.M. Cline, Z. Liu and W. Xue, *Millicharged atomic dark matter*, *Phys. Rev.* **D 85** (2012) 101302 [arXiv:1201.4858] [INSPIRE].

[11] F.-Y. Cyr-Racine and K. Sigurdson, *Cosmology of atomic dark matter*, *Phys. Rev.* **D 87** (2013) 103515 [arXiv:1209.5752] [INSPIRE].

[12] S. Andreas, M.D. Goodsell and A. Ringwald, *Hidden photons in connection to dark matter*, *AIP Conf. Proc.* **1563** (2013) 114 [arXiv:1306.1168] [INSPIRE].

[13] K. Petraki, L. Pearce and A. Kusenko, *Self-interacting asymmetric dark matter coupled to a light massive dark photon*, *JCAP* **07** (2014) 039 [arXiv:1403.1077] [INSPIRE].

[14] K.-W. Ng, H. Tu and T.-C. Yuan, *Dark photons as fractional cosmic neutrino masquerader*, *JCAP* **09** (2014) 035 [arXiv:1406.1993] [INSPIRE].

[15] H. Davoudiasl, H.-S. Lee and W.J. Marciano, *'Dark' Z implications for parity violation, rare meson decays and Higgs physics*, *Phys. Rev.* **D 85** (2012) 115019 [arXiv:1203.2947] [INSPIRE].

[16] PAMELA collaboration, O. Adriani et al., *An anomalous positron abundance in cosmic rays with energies 1.5–100 GeV*, *Nature* **458** (2009) 607 [arXiv:0810.4995] [INSPIRE].

[17] D. Kazanas, R.N. Mohapatra, S. Nussinov, V.L. Teplitz and Y. Zhang, *Supernova bounds on the dark photon using its electromagnetic decay*, *Nucl. Phys.* **B 890** (2014) 17 [arXiv:1410.0221] [INSPIRE].

[18] R. Foot and S. Vagnozzi, *Dissipative hidden sector dark matter*, *Phys. Rev.* **D 91** (2015) 023512 [`arXiv:1409.7174`] [ɪɴSPIRE].

[19] H. An, M. Pospelov, J. Pradler and A. Ritz, *Direct detection constraints on dark photon dark matter*, `arXiv:1412.8378` [ɪɴSPIRE].

[20] BaBar collaboration, J.P. Lees et al., *Search for a dark photon in e^+e^- collisions at BaBar*, *Phys. Rev. Lett.* **113** (2014) 201801 [`arXiv:1406.2980`] [ɪɴSPIRE].

[21] O. Moreno, *The heavy photon search experiment at Jefferson Lab*, `arXiv:1310.2060` [ɪɴSPIRE].

[22] PHENIX collaboration, A. Adare et al., *Search for dark photons from neutral meson decays in $p + p$ and $d + Au$ collisions at $\sqrt{s_{NN}} = 200\,GeV$*, *Phys. Rev.* **C 91** (2015) 031901 [`arXiv:1409.0851`] [ɪɴSPIRE].

[23] W.-S. Hou, M. Kohda and F. Xu, *Measuring the fourth generation $b \to s$ quadrangle at the LHC*, *Phys. Rev.* **D 84** (2011) 094027 [`arXiv:1107.2343`] [ɪɴSPIRE].

[24] LHCb collaboration, *Differential branching fraction and angular analysis of the decay $B^0 \to K^{*0}\mu^+\mu^-$*, *JHEP* **08** (2013) 131 [`arXiv:1304.6325`] [ɪɴSPIRE].

[25] S.D. Aristizabal, F. Staub and A. Vicente, *Shedding light on the $b \to s$ anomalies with a dark sector*, `arXiv:1503.06077` [ɪɴSPIRE].

[26] H. Ruegg and M. Ruiz-Altaba, *The Stueckelberg field*, *Int. J. Mod. Phys.* **A 19** (2004) 3265 [`hep-th/0304245`] [ɪɴSPIRE].

[27] W.-Z. Feng, G. Shiu, P. Soler and F. Ye, *Building a Stückelberg portal*, *JHEP* **05** (2014) 065 [`arXiv:1401.5890`] [ɪɴSPIRE].

[28] A.J. Buras, *Weak Hamiltonian, CP-violation and rare decays*, `hep-ph/9806471` [ɪɴSPIRE].

[29] CMS and LHCb collaborations, *Observation of the rare $B_s^0 \to \mu^+\mu^-$ decay from the combined analysis of CMS and LHCb data*, *Nature* **522** (2015) 68 [`arXiv:1411.4413`] [ɪɴSPIRE].

[30] W.-S. Hou, M. Kohda and F. Xu, *Implication of possible observation of enhanced $B_d^0 \to \mu^+\mu^-$ decay*, *Phys. Rev.* **D 87** (2013) 094005 [`arXiv:1302.1471`] [ɪɴSPIRE].

[31] K. De Bruyn et al., *Branching ratio measurements of B_s decays*, *Phys. Rev.* **D 86** (2012) 014027 [`arXiv:1204.1735`] [ɪɴSPIRE].

[32] K. De Bruyn et al., *Probing new physics via the $B_s^0 \to \mu^+\mu^-$ effective lifetime*, *Phys. Rev. Lett.* **109** (2012) 041801 [`arXiv:1204.1737`] [ɪɴSPIRE].

[33] A.J. Buras, R. Fleischer, J. Girrbach and R. Knegjens, *Probing new physics with the $B_s \to \mu^+\mu^-$ time-dependent rate*, *JHEP* **07** (2013) 077 [`arXiv:1303.3820`] [ɪɴSPIRE].

[34] CMS and LHCb collaborations, *Combination of results on the rare decays $B_{(s)}^0 \to \mu^+\mu^-$ from the CMS and LHCb experiments*, CMS-PAS-BPH-13-007, LHCb-CONF-2013-012 (2014).

[35] HEAVY FLAVOR AVERAGING GROUP collaboration, Y. Amhis et al., *Averages of b-hadron, c-hadron and τ-lepton properties as of early 2012*, `arXiv:1207.1158` [ɪɴSPIRE].

[36] A.J. Buras, F. De Fazio and J. Girrbach, *331 models facing new $b \to s\mu^+\mu^-$ data*, *JHEP* **02** (2014) 112 [`arXiv:1311.6729`] [ɪɴSPIRE].

[37] W. Altmannshofer, P. Paradisi and D.M. Straub, *Model-independent constraints on new physics in $b \to s$ transitions*, *JHEP* **04** (2012) 008 [`arXiv:1111.1257`] [ɪɴSPIRE].

[38] D.M. Straub, *Constraints on new physics from rare (semi-)leptonic B decays*, arXiv:1305.5704 [INSPIRE].

[39] G. Isidori and R. Unterdorfer, *On the short distance constraints from $K_{L,S} \to \mu^+\mu^-$*, *JHEP* **01** (2004) 009 [hep-ph/0311084] [INSPIRE].

[40] A.J. Buras et al., *Patterns of flavour violation in the presence of a fourth generation of quarks and leptons*, *JHEP* **09** (2010) 106 [arXiv:1002.2126] [INSPIRE].

[41] M. Gorbahn and U. Haisch, *Charm-quark contribution to $K_L \to \mu^+\mu^-$ at next-to-next-to-leading order*, *Phys. Rev. Lett.* **97** (2006) 122002 [hep-ph/0605203] [INSPIRE].

[42] A.J. Buras and J. Girrbach, *Towards the identification of new physics through quark flavour violating processes*, *Rept. Prog. Phys.* **77** (2014) 086201 [arXiv:1306.3775] [INSPIRE].

[43] G. Buchalla, A.J. Buras and M.K. Harlander, *Penguin box expansion: flavor changing neutral current processes and a heavy top quark*, *Nucl. Phys.* **B 349** (1991) 1 [INSPIRE].

[44] A.J. Buras, F. De Fazio and J. Girrbach, *$\Delta I = 1/2$ rule, ε'/ε and $K \to \pi\nu\bar{\nu}$ in $Z'(Z)$ and G' models with FCNC quark couplings*, *Eur. Phys. J.* **C 74** (2014) 2950 [arXiv:1404.3824] [INSPIRE].

[45] V. Cirigliano, A. Pich, G. Ecker and H. Neufeld, *Isospin violation in ϵ'*, *Phys. Rev. Lett.* **91** (2003) 162001 [hep-ph/0307030] [INSPIRE].

[46] PARTICLE DATA GROUP collaboration, K.A. Olive et al., *Review of particle physics*, *Chin. Phys.* **C 38** (2014) 090001 [INSPIRE].

[47] T. Blum et al., *Lattice determination of the $K \to (\pi\pi)_{I=2}$ decay amplitude A_2*, *Phys. Rev.* **D 86** (2012) 074513 [arXiv:1206.5142] [INSPIRE].

[48] G. 't Hooft and M.J.G. Veltman, *Scalar one loop integrals*, *Nucl. Phys.* **B 153** (1979) 365 [INSPIRE].